

A Compact Sensor Based on Near Infrared Absorption Spectroscopy for Flow Diagnostics in a Low Density Hydrogen and Oxygen Combustion Driven Shock Tube

X.L. YU*, F. LI, L.H. CHEN, AND X.Y. CHANG

*Key Laboratory of High Temperature Gas Dynamics, Institute of Mechanics,
Chinese Academy of Sciences, Beijing 100190, China*

A water vapour absorption-based fast-response tunable diode laser (TDL) sensor is developed for flow diagnostics in low density hydrogen and oxygen combustion driven shock tubes. The absorption system was operated in the rapid time-division-multiplexing (TDM) wavelength scanning mode to probe two water vapour absorption features at repetition rate up to 45.5 kHz. Temperature was determined from the ratio of the integrated absorbance of the two individual transitions near 7185.597 and 7168.437 cm^{-1} , which have high sensitivity of temperature measurement in the range of 500–1300K. Experiments were performed in a 800 mm diameter hydrogen and oxygen combustion driven shock tube. Time resolved temperature and water vapour mole fraction of the driver gas at the fixed position of the test section are provided. Facility test time was also deduced from the non-absorption light intensity signal. The simple data processing and convenient operation made the sensor became a potential routine application for low density shock tube/tunnel.

Keywords: Tunable diode laser absorption spectroscopy (TDLAS), combustion, rapid time-division-multiplexing (TDM), temperature, water vapour concentration, low density shock tube

1 INTRODUCTION

Applications of near infrared tunable diode lasers (TDL) to combustion and flow diagnostics in impulse facilities continues to appear in the scientific

*Corresponding author: xlyu@imech.ac.cn

literature over the past two decades [1-6]. These sensors have been used successfully to provide *in situ* measurements of temperature gas species concentration, velocity, mass flux and pressure in a variety of facilities [3, 5, 7-11]. Most of these TDL sensors are based on direct absorption technique due to the relatively simple interpretation of measurement results. The sensor bandwidth is usually limited to several kHz by the wide laser scanning range needed to reach the non-absorbing wings of the spectroscopic features [12]. This repetition rate is too slow to be applied to the pulsed facilities, so most absorption sensors designed for the shock tube or tunnel based on fix-wavelength strategy. And because of various noise source such as window fouling, turbulent flow field-induced beam steering, chemiluminescent emission, wavelength modulation spectroscopy (WMS) scheme is utilized to improve the signal-to-noise ratio [12-14]. But for WMS scheme, complexity of the system construction and kHz narrow measurement bandwidth makes the extensive application of the sensor difficult to implement.

In this paper application of a tunable diode laser absorption spectroscopy (TDLAS) system with a repetition rate of 45.5 kHz for flow diagnostics in a low density shock tube has been developed. The system configuration features time-division-multiplexing (TDM) wavelength scanning mode for easy system construction and cost reduction consideration. In mentioned system, two signals are alternated in time. Even This lead to measurement uncertainty for rapid change condition due to two absorption signals are not measured simultaneously, simple system construction and convenient data processing are attractive for application to flow diagnostics in large facilities. With the TDLAS system, flow parameters of mixing zone and driver gas of the shock tube are obtained. The experiments not only demonstrated the measurement accuracy and frequency response of the system, but also laid a foundation for the future measurements of other absorbing species such as O_2 , O in the driven gas.

2 THEORY AND LINE PAIR SELECTION

The fundamental equation for absorption spectroscopy is the Beer-Lambert relation. After passing through a uniform absorbing gas, the transmitted intensity of the monochromatic beam, I_v , can be given in this form:

$$I_v = I_{v,0} \exp(-k_v L) \quad (1)$$

Here $I_{v,0}$ represents incident intensity, I_v represents transmission intensity, k_v represents spectral absorption coefficient at light frequency v (cm^{-1}).

For an isolated absorption transition, the spectral absorption coefficient, k_v (cm^{-1}), is the product of the total pressure of the gas, P (atm), the mole frac-

tion of the absorbing species, X , the line strength, $S(T)$ ($\text{cm}^{-2}\text{atm}^{-1}$), and the line shape function, $\phi(\nu)$ (cm), (defined as $\int \phi(\nu) d\nu = 1$):

$$K_\nu = P \cdot X_{H_2O} \cdot S(T) \cdot \phi(\nu) \quad (2)$$

If the wavelength scans strategy is performed, by integrating absorbance over whole wave range, absorbing species partial pressure, PX_{H_2O} , and temperature, T , can be found by probing two absorption features.

The line strength at any temperature, $S(T)$, can be calculated from the known line strength at some reference temperature, $S(T_0)$, using

$$S(T) = S(T_0) \frac{Q(T_0)}{Q(T)} \left(\frac{T_0}{T} \right) \exp \left[-\frac{hcE''}{k} \left(\frac{1}{T} - \frac{1}{T_0} \right) \right] \frac{\left[1 - \exp \left(\frac{-hc\nu_0}{kT} \right) \right]}{\left[1 - \exp \left(\frac{-hc\nu_0}{kT_0} \right) \right]} \quad (3)$$

where Q is the total internal partition function of the molecule, E'' is the lower state energy of the transition, h is Planck's constant, c is the speed of light and k is Boltzmann's constant. The last term in Equation (3) can be negligible at wavelengths below $2.5 \mu\text{m}$ and temperatures below 2500 K [1].

From Equation (2) and Equation(3) we see that for two-line thermometry, R , the ratio of the integrated absorbance of two isolated transitions is a temperature-dependent function:

$$R = \frac{\int_{\nu_1}^{\nu_1'} P \cdot X_{H_2O} \cdot L \cdot S_1(T) \cdot \phi_1(\nu - \nu_{01}) d\nu}{\int_{\nu_2}^{\nu_2'} P \cdot X_{H_2O} \cdot L \cdot S_2(T) \cdot \phi_2(\nu - \nu_{02}) d\nu} = \frac{S_1(T)}{S_2(T)} = \frac{S_1(T_0)}{S_2(T_0)} \exp \left[-\left(\frac{hc}{k} \right) (E_1 - E_2) \left(\frac{1}{T} - \frac{1}{T_0} \right) \right] \quad (4)$$

Once the temperature is acquired, the species concentration can be deduced from the integrated form of Equation (2).

The temperature sensitivity depends on the energy separation of the two absorption lines and is defined as [15]

$$\text{sensitivity} = \frac{dR/R}{dT/T} = \frac{hc}{k} \left| \frac{E_1 - E_2}{T} \right| \quad (5)$$

The line shape function provides important information since it is a function of many parameters such as pressure, species concentration and temperature. In high resolution experiments, spectral line shape is usually described by the

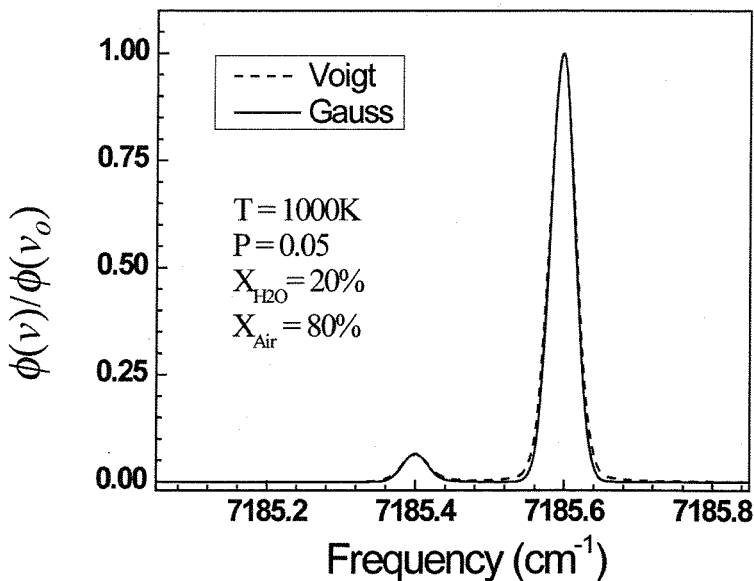


FIGURE 1

Simulated Voigt and Gauss profile of H₂O absorption lines 7185.597cm⁻¹ at T =1000 K, P = 0.05atm, and 20% H₂O in Air

Voigt function which is a convolution of the Gaussian and Lorentz profiles that represent two significant broadening mechanisms.

Under conditions of low pressure ($P \ll 1$ atm), the line shape is dominated by Doppler broadening and the Voigt profile grows into the Gaussian profile, as shown in Figure 1. The simulation of the H₂O transition near 7185.597 cm⁻¹ was implemented at the calculation conditions of $T = 1000$ K, $P = 0.05$ atm, and $X_{\text{H}_2\text{O}} = 20\%$ using spectroscopic parameters provided by HITRAN2004 [16]. As one can see from Figure 1, the difference between the full widths at the half maximum of the Voigt and Gaussian shape was less than 5%.

If the absorption feature can be accurately simulated, fix wavelength technique may be used to reduce costs and improve the measurement bandwidth. The laser frequencies are fixed at the peak absorbance positions. Temperature can be determined from the comparisons of measurement ratio and the simulation one of the two individual absorption lines. Fixed-wavelength direct-absorption strategy does not necessitate scanning of the whole feature, so the sensor bandwidth is only limited to the detector bandwidth which can easily achieve several MHz. But at many experiment conditions, the spectroscopic parameters are unknown, accurately simulation is impossible, therefore calibration experiments are required.

Figure 2(a) illustrates absorption of 20% water vapour in air as a function of pressure near 7185.597 cm⁻¹. It is evident from Figure 2(a) that at pressures

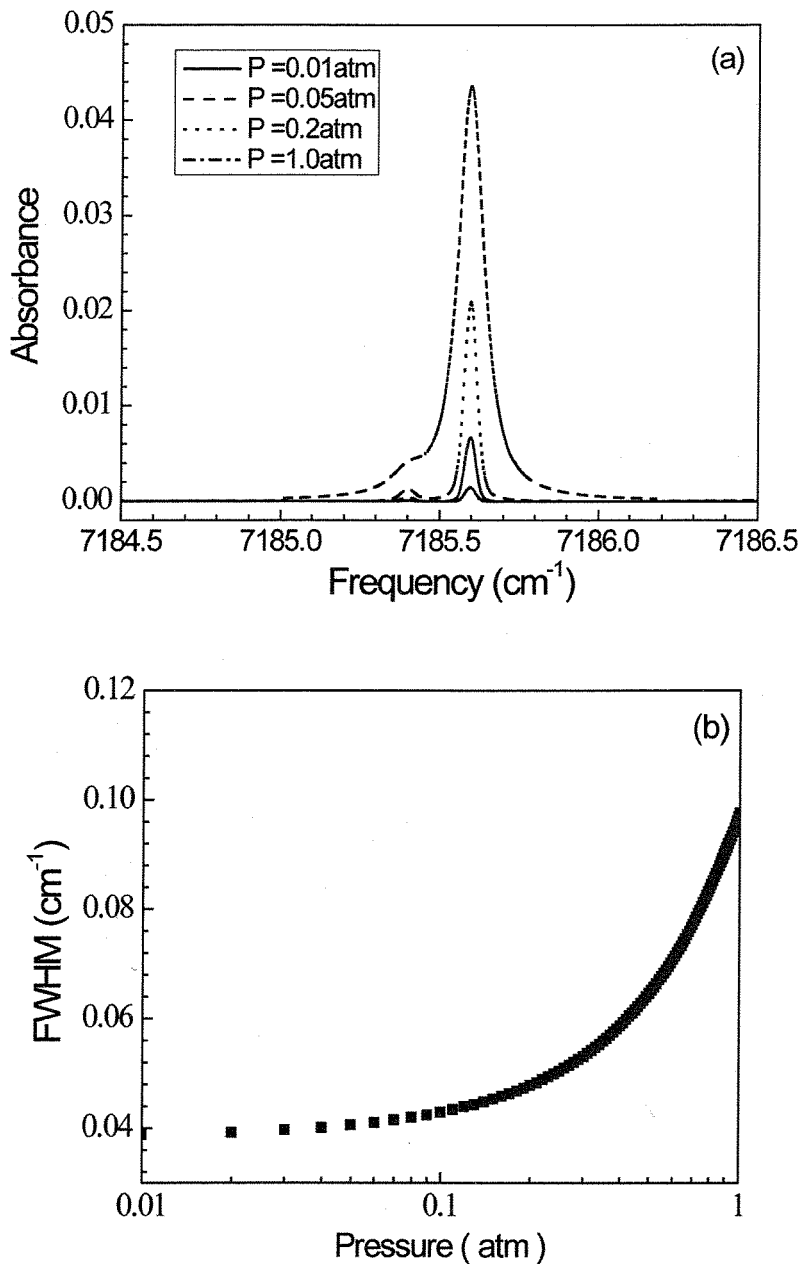


FIGURE 2

(a) Spectral simulation of H_2O absorption near 7185.597 cm^{-1} for different frequencies and (b) full width at half max-high of line 7185.597 cm^{-1} for different pressures. Calculation is based on HITRAN2004 at $T=1000 \text{ K}$, 20% H_2O in air and a 1 cm path length.

higher than 0.2 atm the 7185.597 cm^{-1} absorption line is interfered with by neighbouring weak transitions (at high temperature, mainly spectral line near 7185.401 cm^{-1} , low state energy: 1474.981 cm^{-1}). This will complicate the data processing. Using the wavelength scanning method, the laser fast scan range should be about 15 times the half width of the absorption feature. Figure 2(b) shows the half width of transition 7185.597 cm^{-1} versus pressure. It can be in Figure 2(b) that for line 7185.597 cm^{-1} , at $P=0.05\text{ atm}$, the half width is about 0.05 cm^{-1} and needs a 0.75 cm^{-1} laser scan range. At atmospheric pressure, the half width is about 0.1 cm^{-1} which required laser fast scan range larger than 1.5 cm^{-1} . Different spectral lines have different broadening coefficients, thus some spectral lines may need broader scan range.

The laser fast scan range can be determined by Fabry-Perot Interferometer which usually is used to provide a calibration scan time to laser wavelength. In this paper a commercial Fabry-Perot Interferometer (SA200-12A; Thorlabs, Inc.) with a free spectral range (FSR) of 1.5 GHz was employed to examine the largest fast scan range of lasers at various scan frequency, as shown in Figure 3. These distributed-feedback (DFB) lasers (NLK1E5EAAA; NTT Corp.) we used here are current tuned by a controller (LDC-3724B; ILX Lightwave, Inc.) to lasing near 7185.6 cm^{-1} . Figure 3 shows that laser scan range decreases rapidly as the scan frequency increases. The laser wavelength is tuned over a range larger than 2 cm^{-1} at frequency less than 10 kHz. It is sufficient for measurements at atmosphere pressure. But at 100 kHz frequency, the fast tuned range decreases to 0.85 cm^{-1} , which is only suitable to

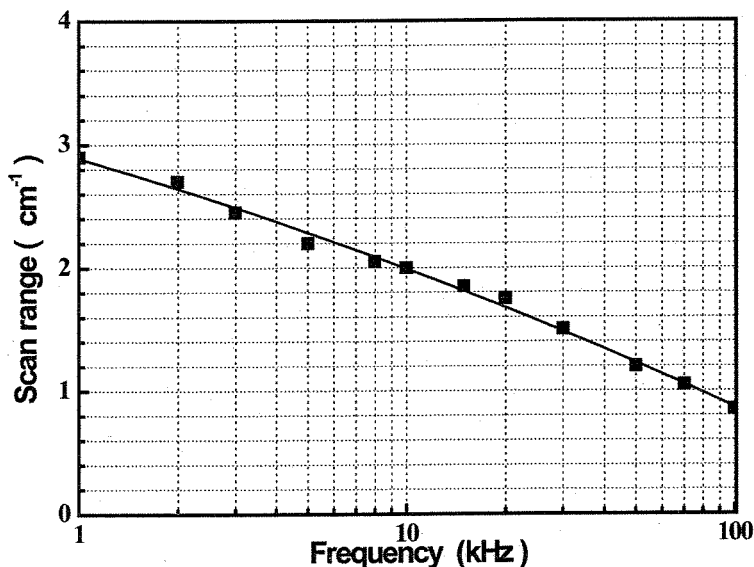


FIGURE 3

The scan range of the DFB laser *versus* scan rate for the selected line position.

low pressure application. As the tuned range decreases, it is impossible to scanning the whole absorption feature in high pressure gas. At this state, only fixed-wavelength strategy is feasible.

From what has been mentioned above, we can come to the conclusion that the match between fast current modulation characteristic of the laser and the parameters in the target flow field (such as pressure, temperature and broadening coefficient of various species) limits the maximum scan rate. When the other parameters are fixed, the lower the pressure, the maximum tuned frequency will be faster. For the low density shock tube we used in this paper, the maximum scan frequency is about 100 kHz.

In absorption based two-line thermometry, the selection of the line pair is very important. Water vapour transitions near 1393 nm are well known, the fundamental spectroscopic parameters in this region have been validated by many researchers. Thus the 140 water vapour absorption lines in the 1389 to 1396 nm region are considered.

Before selecting, we should analyse the region of gas flow parameters. In our experiments, the absorption length is fixed at 80 cm, pressure after the strong shock wave is between 0.03 to 0.1 atm, temperature: 500 to 1500 K, and the mole fraction of water vapour is around 20%. The rules of selection of the line pair adopted here was as used by Zhou *et al* [15]. Spectral calculation in the target region is proceeded with HITRAN2004 to help choosing the transitions. Because the large scale facility we used may cause high noise, we impose lower bound on the peak absorbance should not less than 0.1. A high lower state energy difference is desired to have high temperature sensitivity [17]. One pair absorption lines with wave number 7168.437 and 7185.597 cm^{-1} are reserved. Figure 4 shows individual line shapes about selected line pair. Figure 4 also shows free of interference from nearby lines.

Figure 5(a) shows the line strengths of the line pair *versus* temperature. In the temperature region we are interested in, the similar absorption strength of the two lines would ensure the similar signal-to-noise (S/N) ratio in the experiments. On the other hand, as presented in Figure 5(b), the line pair have high sensitivity of temperature measurement in the 500 to 1300 K range and measurement accuracy was validated by comparison with a thermocouple results in a CH_4/air Mckenna flat burner [18].

3 FACILITY AND EXPERIMENTAL SET-UP

A schematic diagram of experimental set-up is shown in Figure 6. The facility is a variable cross-section stainless-steel shock tube with total length 20 m. The high pressure section of the shock tube was 1.6 m in length and 223 mm in diameter, and the test section was 800 mm in diameter. The measurement location was 14 m downstream from the diaphragm. The shock tube was driven by hydrogen and oxygen combustion with a driver pressure of 30

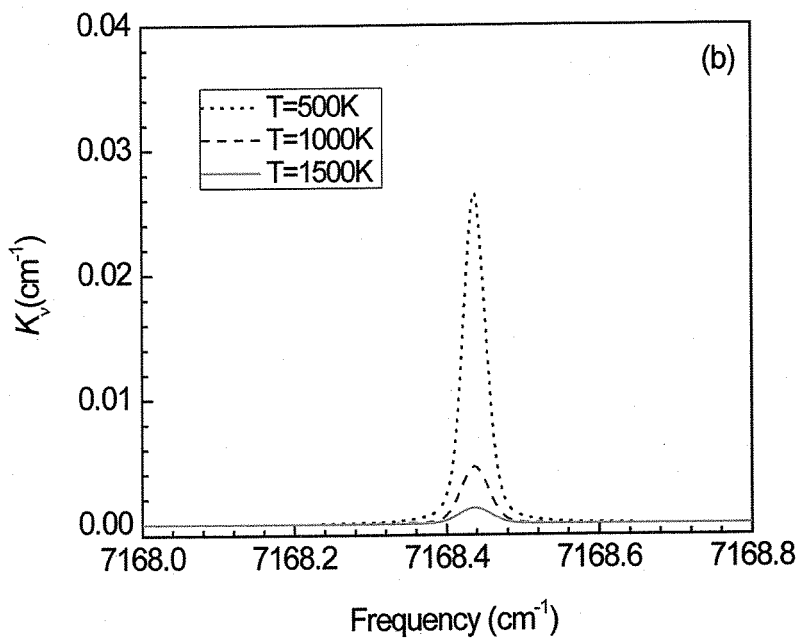
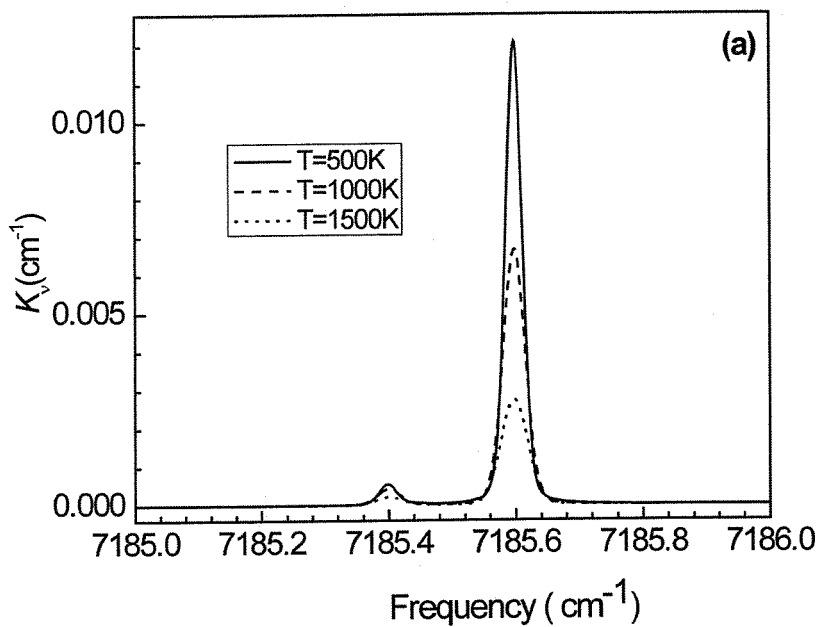


FIGURE 4

The individual shape about the selected line pair for different temperatures at (a) 7185.597 cm^{-1} and (b) 7168.437 cm^{-1} .

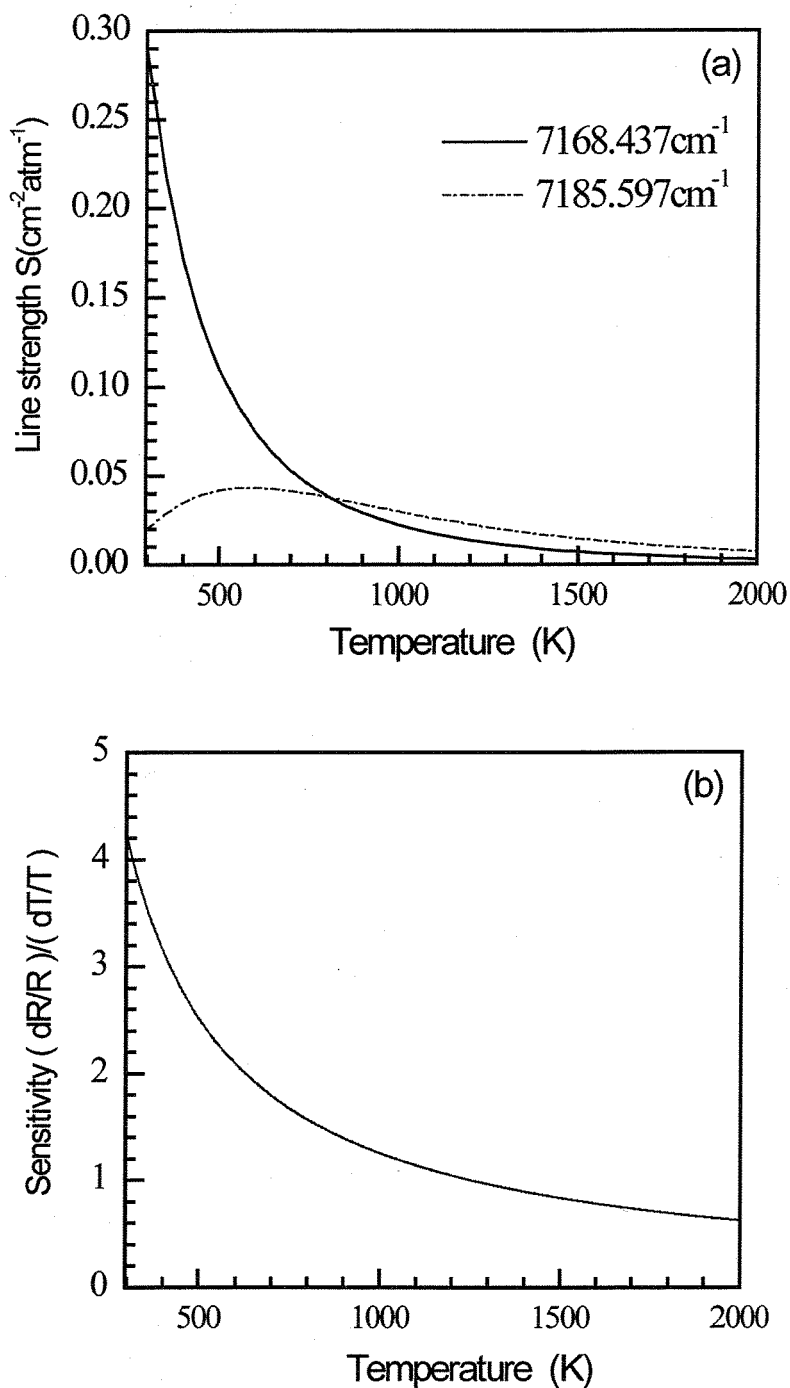


FIGURE 5

(a) Line strength of selected water vapour absorption pairs *versus* temperature and (b) temperature sensitivity of the line pair *versus* temperature.

to 80 atm. The initial pressure in the test section can be set from 1.33 to 133 Pa [19]. With a 2 mm thickness aluminium diaphragm the tube can produce stable shock wave with speed of 2.5 to 7 km/s ($Ma = 8$ to 20). Three ion probes, which are denoted as No. 1, No. 2 and No. 3, were installed to detect the shock arrival for shock speed measurement, and the No. 3 probe is located at the same cross-section with the light transmission path.

The wavelength of two DFB diode lasers, with 10 mW power level and an effective spectral line width (FWHM) of approximately 10 MHz, can be tuned through changing the temperature and current of the diode laser controllers. Fixed temperature control parameter was used to tune the wavelength of the laser into the region of the selected transitions, while wavelength scan was carried out by external current modulation to the controller using a ramp signal from dual channel signal generation (AFG 3022B; Tektronix, Inc.). The two beams are multiplexed into a single-mode fibre by a 1×2 coupler. A collimator (F220FC-C; Thorlabs, Inc.) was used to adjust the beam across the quartz windows on the both sides of the tube. Transmission light is focused by a lens onto an infrared-sensitive 2 mm diameter InGaAs detector with a measurement bandwidth no less than 20 MHz and the output voltage signal was recorded by a memory oscilloscope (DPO4032; Tektronix, Inc.) with 250 MS/s sampling rate. The optics, collimator, windows and detector were enwrapped with plastic bags purged by dry N_2 to avoid interfering absorption by ambient water vapour in the air along the optical path. The lens in front of the detector is necessary because it could provide a larger target for the collection of light in the presence of various beam-steering and misalignment [20].

A TDM wavelength scanned mode [18, 21] was used. The 180° phase difference two half-ramp-waves, which were modulated by square waves, were used to modulate the two laser controllers, respectively. Existed phase difference makes the two lasers be modulated alternately in time. This means only one diode lasers is scanned and emitted at a time, while the other is scanned and emitted at another time.

Figure 6 also shows a schematic of the flow in shock tube. The real line between 1 and 2 shows the motion of the strong shock wave. Region 1 means the initial low pressure section before the shock arrival. Region 2 is the driven gas behind the shock wave. Region 3 is the driver gas from the high pressure section. Turbulent mixing zone exists between driver and driven gas determined by equal velocity and equal pressure on both sides.

4 DATA PROCESSING

Figure 7 shows the raw data of TDM wavelength-scanned direct-absorption result. As one can see from Figure 7, there are two ramps in every period - the smaller one presents the scan of transition 7168.437 cm^{-1} and the larger one

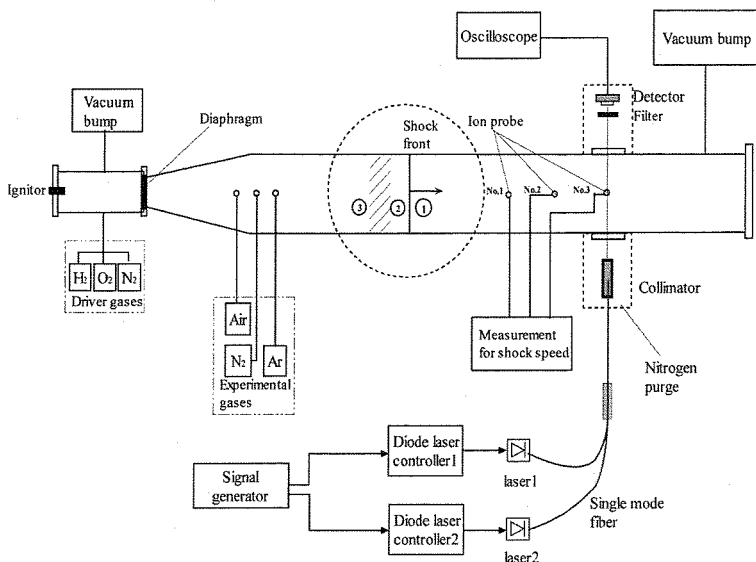


FIGURE 6

Schematic diagram of the experimental set-up of the 800 mm diameter shock tube and the optical instruments arrangement.

corresponds to absorption line 7185.597 cm^{-1} . Though the same voltage ranges of the modulation signal are used, but because of different changed value for output power according to per current at different setting temperature, the transmitted intensity for each laser is different. Figure 7 is drawn at the exact time when Region 2 is ending and the mixing zone is arriving; at that moment the absorbance is increasing which shows that the water vapour is increasing.

The data processing procedure is usually following the sequence: first, intercepts the non-absorbing wings; then, fits the baseline, constructs the absorbance plot of the absorption feature; and finally, fits the absorption feature. In order to simplify the data processing, we fit the absorption feature and the baseline simultaneously, as shown in Figure 7. As discussed in Section 1.2; under conditions of high temperature and low pressure ($P \ll 1 \text{ atm}$) the Voigt profile grows into the Gaussian profile. In this paper all baselines are fitted with a third-order polynomial and a Gaussian profile is used to fit the line shape of the target transition. This will introduce an error of less than 3% to integrate absorbance as a result of neglect of the Lorentz broadening contribution. A post-processing procedure is written to fit the raw data and extract the integrate absorbance and determine temperature and water concentration continuously. This will greatly shorten the time needed and lay a foundation for popularizing the sensor for the normal application.

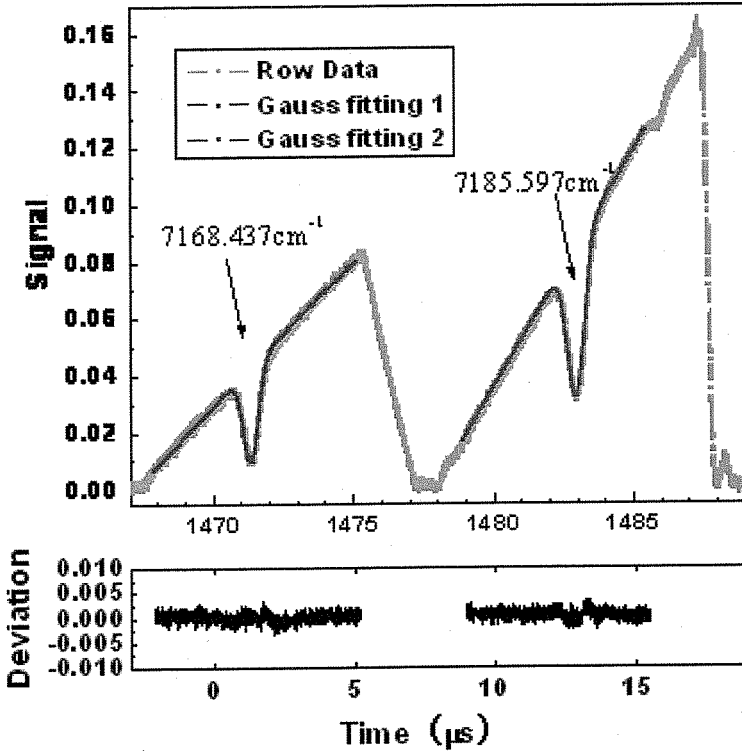


FIGURE 7

Graph showing the fitting of absorption feature and baseline.

5 RESULTS AND DISCUSSION

5.1 Early stage absorption and test time estimation

The experiment parameters in Figure 8 are $P_1 = 0.1$ Torr, $U_s = 5.19$ km/s. Before ignition, oxygen and hydrogen in the driver section are at 0.4 atm and 3.4 atm, respectively. In Figure 8(a) a sharp rising voltage output of the No. 3 ion probe is evident, indicating the arrival of the shock at the station of No. 3 probe location in the time t_1 and propagates to the downstream region of the tube. Behind the shock front there is partial dissociated hot air. Due to the turbulent mixing effect, the gases in Region 3 intrudes into the region behind shock front. This effect blurs the interface between Region 3 and Region 2 and forms the zone which contain gases from Region 2 and driver gases; thus the available test time is greatly decreased. Even the output signal of No. 3 ion probe is still high at time t_2 in Figure 8(a) - the appearance of absorption indicates the existence of water vapour. Moreover, for the test condition, the calculated temperature behind shock front is about 5130 K and in this state

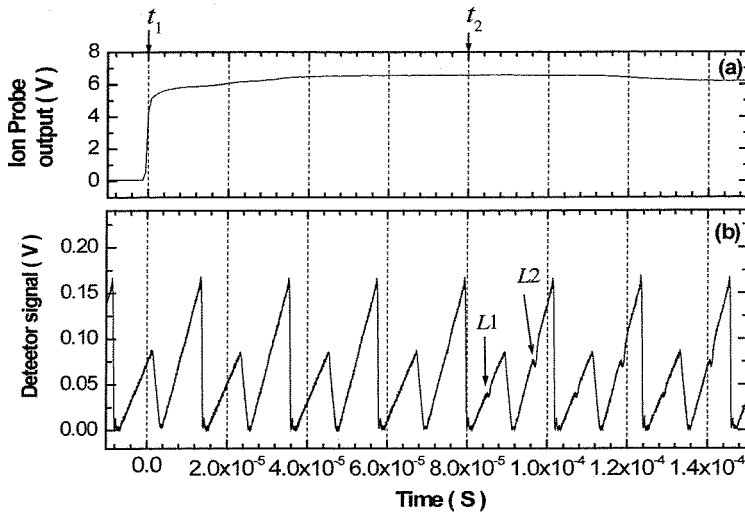


FIGURE 8

(a) Ion probe output *versus* time and (b) corresponding absorption signal *versus* time under test conditions of $P_1 = 0.1$ Torr and $U_s = 5.19$ km/s.

the water vapour will be fully dissociated into atomic hydrogen and hydroxyl radical. As such, the appearance of absorption also means sharp temperature decrease of gases. The best way to accurately measure the actual test time is possible to monitor radiation from atomic hydrogen, hydroxyl radical by means of optical emission spectroscopy, or measure ultraviolet absorption of hydroxyl radical for accurately concentration determination in the wavelength of OH(A-X) resonant transition.

5.2 Flow parameters of mixing region and Region 3

Because the gas in Region 2 is the high temperature ionization air without water vapour, absorption in there can be neglected. So, the TDLAS sensor based on water vapour absorption is inability to measure the rotational temperature of the driven gas in the region. Till the mixing zone arrival, water vapour occurs at the measurement cross-section, absorbing arising, temperature and concentration can be gotten. The running state of the gas after Region 2 can be analysed by the temperature and water concentration variety.

As mentioned above, raw data is converted to time-resolved temperature and water vapour concentration data by the data processing. Figure 9 shows the typical results of measurement. Figure 9(a) presents output signal of No. 3 ion probe *versus* time and Figure 9(b) presents the H_2O molecule number density and temperature *versus* time. Based on the relationship of the shock wave in high Mach number shock tube, the temperature pressure and the

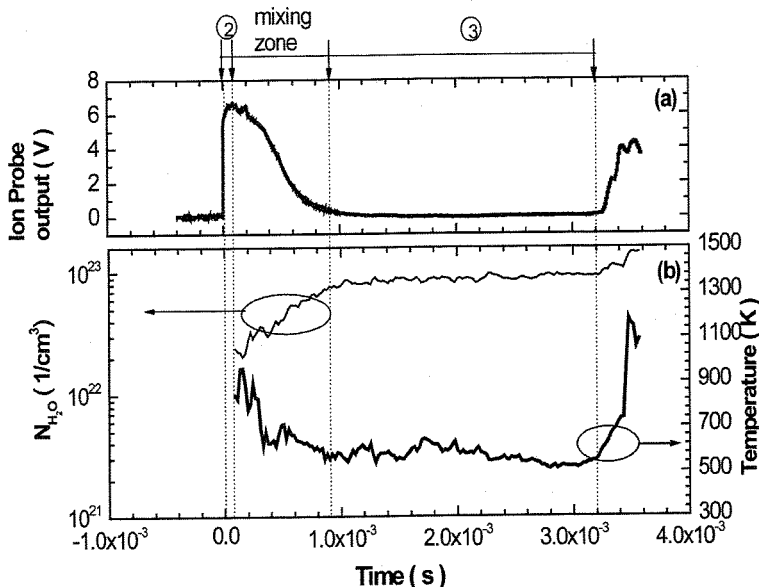


FIGURE 9

Typical time-resolved results for the TDLAS system: (a) the voltage signal of ionization probe No. 3 and (b) measured temperature and molecule number density *versus* time under test conditions of $P_1 = 0.1$ Torr and $U_s = 5.19$ km/s.

velocity of the driven gas behind shock can be obtained: $P_2 = 0.0359$ atm and $T_2 = 5130$ K.

One can see from Figure 9 that in the mixing zone, water vapour content increases gradually, reflecting the turbulent mixing of the driver and driven gas which is one of the primary causations reducing the facility test time. Also because of turbulent mixing, temperature decreases slowly and becomes stable after 1 ms which means Region 3 starts. Then the rarefaction wave arrives moving from the divergent section which cause the temperature decreasing and concentration increasing. At a time of around 3.3 ms the reflected shock wave arrives, temperature and concentration increase greatly. But because of the effect of the special configuration of the back wall, the reflected shock wave is not an ideal wave front. It is difficult to give a quantitative analysis.

For lower Mach number conditions, reflected expansion fan of the wall in the high pressure region and the waves generate in the divergent section will catch up the mixing zone soon.; therefore it is difficult to analyse Region 3 using shock tube theory. Two-dimensional computational fluid dynamic (CFD) simulations would give a better understanding of the flow states. The TDLAS sensor data can suitable be used to comparison with the CFD results.

The typical test time of the shock tube with high Mach number is on the order of hundreds microseconds. The period of our sensor is 22 ms, which is incapable of use in such pulsed facilities. But, for the shock tube or tunnel with lower Mach number which has longer test time (on the order of milliseconds), the measurement system will be more suitable.

For the low density condition we used here, it is feasible to use the Gaussian profile to fit the absorption line shape instead of Voigt profile; however, the Lorentzian broadening contribution cannot be neglect in higher pressure applications.

Isolated absorption lines will be profuse in low pressure absorption. It will be practicable to scan over a pair of transitions using a single diode laser [17]. With this mind, the TDLAS system will be simplified and measurement frequency will be doubled. The subsequent work will be done following this thought.

6 CONCLUSIONS

A sensor based on tunable diode laser absorption spectroscopy (TDLAS) has been constructed for temperature and water vapour concentration measurement. Two water vapour absorption transitions near 1393 nm (7168.437 and 7185.597 cm^{-1}) were selected and analysed using spectrum database HITRAN2004. Time-division-multiplexing (TDM) scanned-wavelength direct absorption strategy was utilized at near 45 kHz scan rate. Successful measurement has been done in a 800 mm diameter low density shock tube driven by hydrogen and oxygen combustion. Test time of Region 2, temperature and water concentration in the mixing zone and Region 3 were acquired. This information is helpful to understand the running state of the variable cross-section shock tube and provided verification data for computational fluid dynamic (CFD) simulation.

ACKNOWLEDGEMENTS

The work is partially supported by the National Science Foundation of China (Grant No. 10772188 and Grant No. 10525212). The authors thank professor N.Y. Zhu for kindly discussing this work and acknowledge the technical assistance provided by Ms. L.S. Huang of the Institute of Mechanics.

REFERENCES

- [1] Allen M.G., Diode laser absorption sensors for gas-dynamic and combustion flows. *Measurement Science and Technology* **9**(4) (1998), 545-562.

- [2] Docquier N. and Candel S. Combustion control and sensors: A review. *Progress in Energy and Combustion Science* **28**(2) (2002), 107-150.
- [3] Philippe L.C. and Hanson R.K. Laser-diode wavelength-modulation spectroscopy for simultaneous measurement of temperature, pressure and velocity in shock heated oxygen flows. *Applied Optics* **32**(30) (1993), 6090-6103.
- [4] Bryner E.B., Diskin G.S., Goynes C.P., McDaniel J.C., Krauss R.H. and Slate T.A. Water vapour concentration measurement in high enthalpy flows using infrared absorption. *39th AIAA/ASME/SAE/ASEE Joint Propulsion Conference and Exhibition*. 20-23 July 2003, Huntsville, AL., USA. AIAA-2003-4580.
- [5] Chen S.J., Silver J.A. and Bomse D.S. Combustion species sensor for scramjet flight instrumentation. *41st AIAA/ASME/SAE/ASEE Joint Propulsion Conference and Exhibition*. 10-13 July 2005, Tucson, AZ., USA. AIAA-2005-3574.
- [6] Liu X., Jeffries J.B., Hanson R.K., Hinckley K.M. and Woodmansee M.A. Development of a tunable diode laser sensor for measurements of gas turbine exhaust temperature. *Applied Physics B: Lasers and Optics* **82**(3) (2006), 469-478.
- [7] Richter D., Lancaster D.G. and Tittel F.K. Development of an automated diode-laser-based multicomponent gas sensor. *Applied Optics* **39**(24) (2000), 4444-4450.
- [8] Teichert H., Fernholz T. and Ebert V. Simultaneous *in situ* measurement of CO, H₂O and gas temperatures in a full-sized coal-fired power plant by near-infrared diode lasers. *Applied Optics* **42**(12) (2003), 2043-2051.
- [9] Farooq A., Jeffries J.B. and Hanson R.K. CO₂ concentration and temperature sensor for combustion gases using diode-laser absorption near 2.7 μ m. *Applied Physics B: Lasers and Optics* **90**(3-4) (2008), 618-628.
- [10] Sanders S.T., Mattison D.W., Jeffries J.B. and Hanson R.K. Time-of-flight diode-laser velocimeter using a locally seeded atomic absorber: Application in a pulse detonation engine. *Shock Wave* **12**(6) (2003), 435-441.
- [11] Upschulte B.L., Sonnenfroh D.M. and Allen M.G.. Measurements of CO, CO₂, OH and H₂O in room temperature and combustion gases using a broadly current-tuned multi-section InGaAsP diode laser. *Applied Optics* **38**(9) (1999), 1506-1512.
- [12] Li H., Farooq A., Jeffries J.B. and Hanson R.K. Near-infrared diode laser absorption sensor for rapid measurements of temperature and water vapour in a shock tube. *Applied Physics B: Lasers and Optics* **89**(2) (2007), 407-416.
- [13] Arroyo M.P., Langlios S. and Hanson R.K. Diode-laser absorption technique for simultaneous measurements of multiple gas dynamic parameters in high-speed flows containing water vapour. *Applied Optics* **33**(15) (1994), 3296-3307.
- [14] Cavolowsky J.A., Newfield M.E. and Loomis M.P. Laser absorption measurements of OH concentration and temperature in pulsed facilities. *AIAA Journal* **31**(3) (1993), 491-498.
- [15] Zhou X., Liu X., Jeffries J.B. and Hanson R.K. Development of a sensor for temperature and water vapour concentration in combustion gases using a single tunable diode laser. *Measurement Science and Technology* **14**(8) (2003), 1459-1468.
- [16] Rothman L.S., Jacquemart D., Barbe A., Benner D., Birk M., Brown L.R., Carleer M.R., Chackerian C.J., Chance K., Coudert L.H., Dana V., Devi V.M., Flaud J.M., Gamache R.R., Goldman A., Hartmann J.M., Jucks K.W., Maki A.G., Mandin J.Y. and Massie S.T. The HITRAN2004 molecular spectroscopic database. *Journal of Quantitative Spectroscopy and Radiative Transfer* **96**(2) (2005), 139-204.
- [17] Zhou X., Jeffries J.B. and Hanson R.K. Development of a fast temperature sensor for combustion gases using a single tunable diode laser. *Applied Physics B: Lasers and Optics* **81**(5) (2005), 711-722.
- [18] Yu X.L., Li F., Chen L.H. and Chang X.Y. A tunable diode-laser absorption spectroscopy (TDLAS) thermometry for combustion diagnostics. *15th AIAA International Space Planes and Hypersonic Systems and Technologies Conference*. 28 April-1 May 2008, Dayton, OH., USA. AIAA-2008-2657.

- [19] Zhu N.Y., Yang Q.S., Zhang H.L., Yu X.L. and Huang L.S. Investigation on nonequilibrium radiation and relaxation phenomena in shock tubes. *Acta Mechanica Sinica* **19**(1) (2003), 46-51.
- [20] Liu J.T.C., Rieker G.B., Jeffries J.B., Gruber M.R., Carter C.D., Mathur T. and Hanson R.K. Near-infrared diode laser absorption diagnostic for temperature and water vapour in a scramjet combustor. *Applied Optics* **44**(31) (2005), 6701-6711.
- [21] Griffiths A.D. and Houwing A.F.P. Diode laser absorption spectroscopy of water vapour in a scramjet combustor. *Applied Optics* **44**(31) (2005), 6653-6659.